

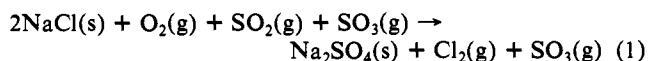
# Mechanism for Forming Sodium Pyrosulfate from Sodium Chloride, Sulfur Dioxide, and Oxygen

Alfred B. Anderson\* and S. C. Hung

Contribution from the Chemistry Department, Case Western Reserve University, Cleveland, Ohio 44106. Received May 12, 1983

**Abstract:** Energy and reaction pathway calculations show sodium pyrosulfate ( $\text{Na}_2\text{S}_2\text{O}_7$ ) is more stable than sodium sulfate ( $\text{Na}_2\text{SO}_4$ ) +  $\text{SO}_3(\text{g})$ . A common precursor to both products when formed on a NaCl surface is an  $\text{SO}_2 + \text{O}_2$  adduct which transfers an oxygen atom to  $\text{SO}_3$ . A low-energy barrier to this process is reached as the  $\text{O}_2$  bond stretches and two electrons are transferred from chloride in the surface, yielding trigonal-pyramidal  $\text{SO}_4^{2-}$  which has two paths open to it. The lower-energy path has this  $\text{SO}_4^{2-}$  bond to  $\text{SO}_3$  leading to pyrosulfate; the higher-energy path has this  $\text{SO}_4^{2-}$  take the tetrahedral sulfate structure.  $\text{Cl}_2$  leaves the surface after the pyrosulfate or sulfate forms.  $\text{Na}^+$  leaves the surface to bond to the anions. Both anions undergo low activation energy umbrella distortions, yielding tetrahedrally coordinated S. Our results offer strong theoretical support for the experimental results of Fielder, Stearns, and Kohl: specifically, (a) rate is proportional to  $\text{SO}_3$  pressure; (b)  $\text{Na}_2\text{S}_2\text{O}_7$  forms first at lower temperatures; (c)  $\text{Na}_2\text{S}_2\text{O}_7$  decomposes, generating  $\text{Na}_2\text{SO}_4$ ; and (d)  $\text{Na}_2\text{SO}_4$  forms directly at higher temperature. At high temperatures the  $T\Delta S$  contribution is larger than the  $\Delta H$  contribution to  $\Delta G$ , favoring sulfate formation even though it has a greater enthalpy than pyrosulfate at low temperatures.

In a recent study Anderson and Debnath<sup>1</sup> used molecular orbital theory to determine a low-energy pathway for sodium sulfate formation from sodium chloride, oxygen, and sulfur dioxide according to the reaction



In this reaction  $\text{SO}_3$  acts as a catalyst, reacting with a previously studied<sup>2,3</sup> singlet  $\text{SO}_2\text{-O}_2$  adduct near the NaCl surface to abstract O, forming  $\text{SO}_4$  which accepts two electrons and 2  $\text{Na}^+$  from the surface, to yield  $\text{Na}_2\text{SO}_4$ . The other products are  $\text{SO}_3$  and  $\text{Cl}_2$ . A first-order dependence on catalyst ( $\text{SO}_3$ ) concentration and a low 22-kJ/mol reaction barrier determined experimentally by Fielder et al.<sup>4</sup> lend support to the predicted mechanism.

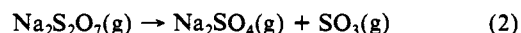
Recent experimental investigations of Kohl et al.<sup>5</sup> show sodium sulfate is not the only possible product. While from 450 to 625 °C  $\text{Na}_2\text{SO}_4$  is the dominant product, at lower temperatures, 400 to 450 °C, sodium pyrosulfate,  $\text{Na}_2\text{S}_2\text{O}_7$ , forms in the molten state. The pyrosulfate anion,  $\text{S}_2\text{O}_7^{2-}$ , is of the form of a symmetric  $\text{SO}_4^{2-} + \text{SO}_3$  adduct which is presumably driven to loss of  $\text{SO}_3(\text{g})$  at higher temperatures due to the entropy increase and its effect on  $\Delta G$  through the  $T\Delta S$  contribution ( $\Delta H$  is obviously positive for the loss process). This new information would appear to be readily explained by a mechanism where at the transition state for reaction 1, ( $\text{O}_2\text{SO}\cdots\text{OSO}_3^{2-}$ ), the O joining  $\text{SO}_3$  carries  $\text{SO}_3$  with it and bonds to the S of the newly-formed  $\text{SO}_3$ . This mechanism is the theme of this study. The same atom superposition and electron delocalization molecular orbital (ASED-MO) theory and the same parameters as in ref 1 are used here.

Sodium sulfate formation under the conditions described above has technological importance. Liquid sodium sulfate forms according to reaction 1 on metal alloy turbine blades where it is a powerful corrosive agent,<sup>6</sup> capable of destroying protective oxide layers, leading to failure by "hot corrosion".<sup>7</sup> Sulfates and pyrosulfates are also important to sulfuric acid formation.

## Results and Discussion

When the  $\text{C}_s$   $\text{SO}_2\text{-O}_2$  adduct forms on the surface it is easily bent to the  $\text{C}_1$  structure in Figure 1 so that it can react with  $\text{SO}_3$  as shown. In ref 1 calculations were performed up to the transition state for O-O bond breaking on a cluster surface model. As shown there, when the O-O bond stretches to the transition state an  $\text{O}_2$   $\Pi^*$  orbital drops low enough in energy to accept electrons from chloride anions in the surface. At this point 2  $\text{Na}^+$  cations join the trigonal-pyramidal  $\text{SO}_4^{2-}$  anion and  $\text{Cl}_2(\text{g})$  leaves the surface. For simplicity, we omitted the surface cluster at this point. The completion of the reaction leading to a tetrahedral  $\text{SO}_4^{2-}$  anion and  $\text{SO}_3(\text{g})$  is shown in the right-hand pathway of Figure 1.

In the present study we have calculated the reaction surface for an alternate reaction shown in the left-hand pathway of Figure 1. The precursor to the transition state has two eclipsed  $\text{SO}_3$  fragments joined to the connecting O with  $\text{Na}^+$  anions placed as shown. For  $\text{Na}_2\text{S}_2\text{O}_7$ , the transition to the final tetrahedral coordination involves a small barrier of 18 kJ/mol compared to 33 kJ/mol for  $\text{SO}_4^{2-}$ . Our (approximate) calculations have the reaction



endothermic by 169 kJ/mol.

Sodium pyrosulfate formation was also studied with  $\text{SO}_3$  fragments at each end staggered. In this case the precursor, transition state, and product were only slightly less stable by the respective amounts 8, 9, and 4 kJ/mol. The structure of  $\text{Na}_2\text{S}_2\text{O}_7$  does not seem to be known experimentally, but an X-ray determination by Lyton and Truter for crystalline  $\text{K}_2\text{S}_2\text{O}_7$ <sup>8</sup> agrees with the eclipsed conformation favored by our calculation. We have assumed a tetrahedral S coordination for simplicity and Lyton and Truter find angles varying from 101.3 to 115.5° (109.5° is the tetrahedral angle). We fixed the three S-O bond lengths at each end to the same value, optimized to be 1.49 Å compared to Lyton and Truter's range of 1.428 to 1.447 Å. Larger differences are found in comparing our calculated inner bridging S-O bond lengths of 1.46 Å and the S-O-S angle of 144° with the Lyton and Truter values of 1.645 Å and 124.2°. Presumably our approximate non-self-consistent theory is letting the  $\text{SO}_3$  fragments with their negative charges get too close together (the central O is nearly neutral). The angle is dependent on these two bond lengths; when they are set to 1.645 Å, the optimal angle is cal-

(1) A. B. Anderson and N. C. Debnath, *J. Phys. Chem.*, **87**, 1938 (1983).

(2) A. B. Anderson, *Chem. Phys. Lett.*, **93**, 538 (1982).

(3) R. Kugel and H. J. Taube, *J. Phys. Chem.*, **79**, 2130 (1975).

(4) W. L. Fielder, C. A. Stearns, F. J. Kohl, and G. C. Fryburg, "Formation of  $\text{Na}_2\text{SO}_4(\text{c})$  from  $\text{NaCl}(\text{c})$ ,  $\text{SO}_2(\text{g})$  and  $\text{O}_2(\text{g})$ ", International Conference on High-Temperature Corrosion, San Diego, CA, March 2-6, 1981.

(5) F. J. Kohl and W. L. Fielder, private communication.

(6) G. C. Fryburg, F. J. Kohl, C. A. Stearns, and W. L. Fielder, *J. Electrochem. Soc.*, **129**, 571 (1982).

(7) J. Stringer, *Annu. Rev. Mater. Sci.*, **7**, 477 (1977).

(8) H. Lyton and M. R. Truter, *J. Chem. Soc., Part 4*, 5112 (1960).

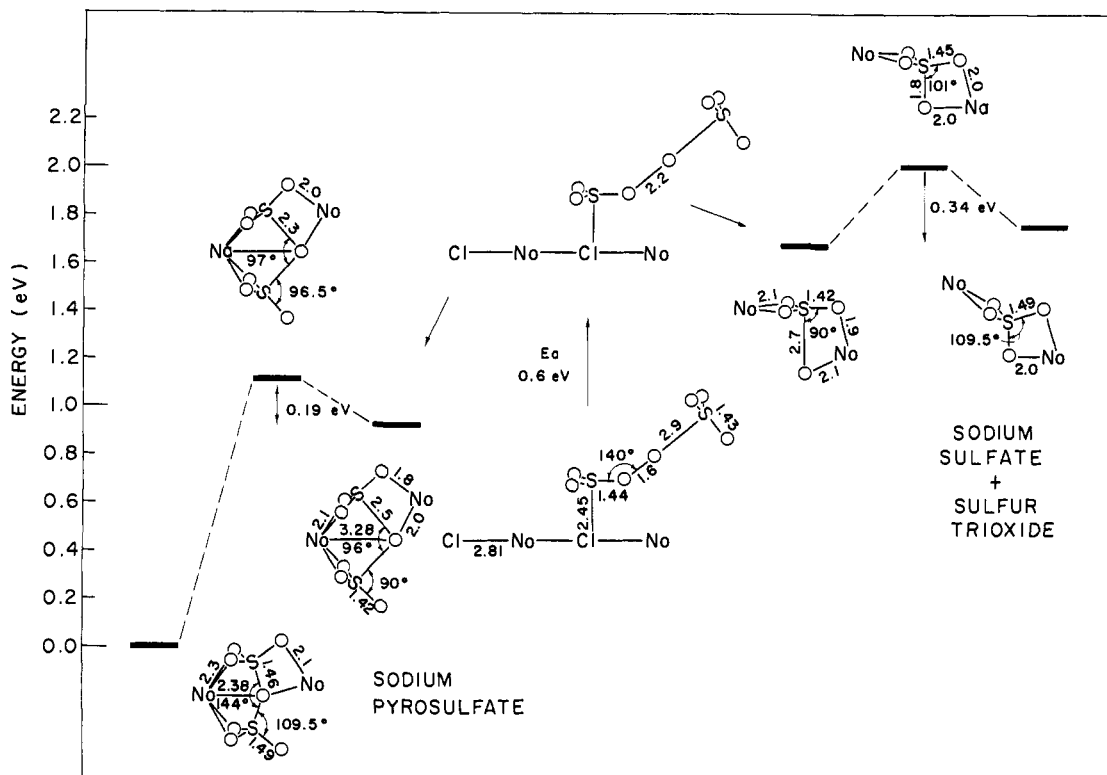


**Figure 1.** The central section shows  $\text{SO}_3$  interacting with  $\text{SO}_2\text{O}_2$  adduct on the  $\text{NaCl}$  surface going to the transition state. After the transition state  $\text{Cl}_2$  and the surface are omitted for simplicity. The energetics and mechanism for  $\text{Na}_2\text{SO}_4 + \text{SO}_3$  formation are on the right.  $\text{Na}_2\text{S}_2\text{O}_7$  formation is shown to the left.

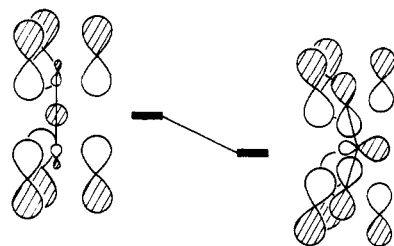


**Figure 2.** Orbital stabilization predominantly responsible for the bent  $\text{S-O-S}$  bond in the pyrosulfate anion.

culated to be  $123.5^\circ$ , agreeing with experiment for solid  $\text{K}_2\text{S}_2\text{O}_7$ .

The  $\text{S-O-S}$  bonding is a consequence of a single orbital becoming stabilized as in Figure 2. On each  $\text{SO}_3$  end the  $1a_2''$   $\Pi$  orbital (ref 1) may be seen to be antibonding to an  $s$  orbital on the central  $\text{O}$  when  $\text{S-O-S}$  is linear. On bending there is  $s$ - $p$  hybridization on the central  $\text{O}$ , allowing bonding stabilization between it and the two  $\text{S}$  atoms. This effect is stronger than the usual Milliken-Walsh explanation of the cause of bending in  $\text{H}_2\text{O}$  where the  $2a_1$  lone-pair orbital is stabilized on bending.<sup>9</sup>

In solid potassium pyrosulfate the anions are shared among cations so it is unlikely that a detailed comparison can be made with cation positions in our sodium pyrosulfate molecule. A general feature may, however, be noted: In  $\text{K}_2\text{S}_2\text{O}_7(\text{s})$  the cations are closely associated with nine oxygens of four anions. In  $\text{Na}_2\text{S}_2\text{O}_7(\text{g})$  we find one  $\text{Na}^+$  is associated with five oxygens and the other with two oxygens. In the staggered form, one  $\text{Na}^+$  is associated with four oxygens and the other with three. Thus the cations want to get as close as they can to the anions for strongest bonding.

The molecular orbital analysis of the anion-cation bonding is shown for sodium sulfate in Figure 3. Two sulfate  $a$  symmetry orbitals are significantly stabilized by overlap with  $\text{Na}$   $s$  orbitals. The lower-orbital stabilization involves a negative overlap, which has been seen in a variety of other studies as well,<sup>10-12</sup> and which

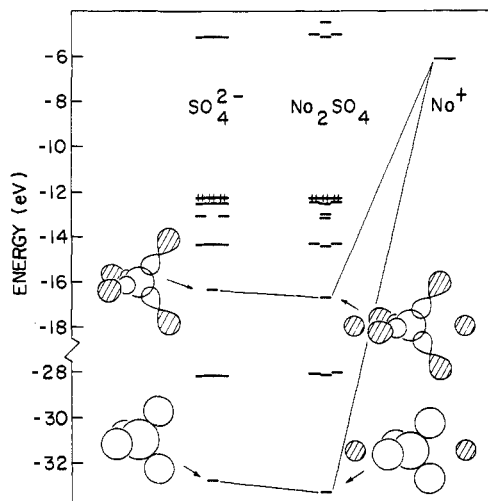
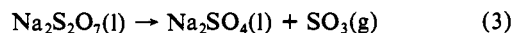


**Figure 3.** Bonding stabilizations between  $\text{Na}^+$  cations and  $\text{SO}_4^{2-}$  anion.

Whangbo and Hoffmann have explained by using the perturbation theory.<sup>11</sup> The upper involves in-phase stabilization. It is reasonable that the most stabilization will be gained in pyrosulfates as well when the cation's orbitals interact with as many constituent atoms in the anion as possible.

We see (Figure 1) that  $\text{Na}_2\text{S}_2\text{O}_7(\text{g})$  is energetically more stable than  $\text{Na}_2\text{SO}_4(\text{g}) + \text{SO}_3(\text{g})$ , which is consistent with experiments showing the pyrosulfate forms at  $400\text{--}450^\circ\text{C}$ .<sup>5</sup> The conversion to sulfate and  $\text{SO}_3(\text{g})$  in the  $450\text{--}625^\circ\text{C}$  range may be understood by appealing to  $\Delta S$  for the reaction



When  $\Delta G = \Delta H - T\Delta S$  is negative, the above reaction will proceed to the right. A thermal decomposition study of Kostin et al.<sup>13</sup>

(10) A. B. Anderson, *J. Catal.*, **67**, 129 (1981).

(11) M.-H. Whangbo and R. Hoffmann, *J. Chem. Phys.*, **68**, 5498 (1978).

(12) C. J. Marsden and L. S. Bartell, *Inorg. Chem.*, **15**, 2713 (1976).

(9) See, for example, B. M. Gimarc, *J. Am. Chem. Soc.*, **93**, 593 (1971).

indicates  $\Delta H^\circ$  is 144 kJ/mol for reaction 3, quite close to our calculated value of 169 kJ/mol for the gas-phase reaction 2. They find, furthermore, a value of 139 J/deg-mol for  $\Delta S^\circ$ .

### Conclusion

Using molecular orbital theory, we have determined reaction mechanisms for sodium sulfate and sodium pyrosulfate formation from solid sodium chloride, sulfur dioxide, and oxygen. The reaction involves a singlet  $\text{SO}_2\cdot\text{O}_2$  intermediate adsorbed to the NaCl surface. Gas-phase  $\text{SO}_3$  abstracts an oxygen atom from  $\text{O}_2$  in the  $\text{SO}_2\cdot\text{O}_2$  adduct, forming  $\text{SO}_4^{2-}$ . As this anion forms  $\text{Na}^+$

cations from the surface bond to it and  $\text{Cl}_2(\text{g})$  desorbs. The anion has two pathways open to it; the lower-energy one has it bonding to the  $\text{SO}_3$  left behind on the surface, forming  $\text{S}_2\text{O}_7^{2-}$ . Both the sulfate and pyrosulfate precursors undergo low-energy umbrella distortions leading to tetrahedral sulfur coordination. Though pyrosulfate is more stable at low temperature, at high temperature it is driven by entropy to lose  $\text{SO}_3$ , yielding sodium sulfate.

**Acknowledgment.** We are warmly appreciative to Drs. William L. Fielder, Fred J. Kohl, and Carl A. Stearns of the NASA Lewis Research Center for advice concerning this work, which has been supported by NASA Grant NAG3-341.

**Registry No.**  $\text{Na}_2\text{S}_2\text{O}_7$ , 13870-29-6; NaCl, 7647-14-5;  $\text{SO}_2$ , 7446-09-5;  $\text{O}_2$ , 7782-44-7;  $\text{SO}_3$ , 7446-11-9.

(13) L. P. Kostin, L. L. Pluzhnikov, and A. N. Ketov, *Russ. J. Phys. chem.*, **49**, 2235 (1975).

## Theoretical Study of the Triple Metal Bond in $d^3$ - $d^3$ Binuclear Complexes of Chromium, Molybdenum, and Tungsten by the Hartree-Fock-Slater Transition State Method

Tom Ziegler

Contribution from the Department of Chemistry, University of Calgary, Calgary, Alberta, Canada T2N 1N4. Received April 25, 1983

**Abstract:** Hartree-Fock-Slater calculations are reported for the two metal fragments  $\text{MoL}_3$  and  $\text{CrL}_3$  with  $L = \text{H}, \text{CH}_3, \text{Cl}, \text{NH}_2,$  and  $\text{OH}$ . The  $\text{ML}_3$  systems all have a trigonal planar geometry with the metal-to-ligand bond strength in the order  $\text{OH} > \text{Cl} > \text{NH}_2 > \text{CH}_3 > \text{H}$ . The bonding energies of  $\text{MoL}_3$  are somewhat larger than the corresponding energies of  $\text{CrL}_3$ . Hartree-Fock-Slater calculations are also reported for the two binuclear systems  $\text{Mo}_2\text{L}_6$  and  $\text{Cr}_2\text{L}_6$  with  $L = \text{H}, \text{CH}_3, \text{Cl}, \text{NH}_2,$  and  $\text{OH}$ . The staggered conformation is the preferred geometry for all the systems. The optimized metal-metal bond distances are calculated to be in the range 2.22 to 2.25 Å for the Mo systems and in the range 1.91 to 1.95 Å for the Cr systems. The strength of the metal-metal bonds follows the order  $\text{Mo-Mo}$  (468-414  $\text{kJ mol}^{-1}$ )  $>$   $\text{Cr-C}$  (301-217  $\text{kJ mol}^{-1}$ ). A study of  $\text{W}_2\text{H}_6$  showed that the inclusion of relativistic effects increased the metal-metal bond energy from 422 to 535  $\text{kJ mol}^{-1}$ .

### 1. Introduction

There has recently been considerable interest in the electronic structure of binuclear  $d^3$ - $d^3$  complexes following the synthesis and structural characterization of several  $\text{M}_2\text{L}_6$  systems<sup>1</sup> with  $M = \text{Mo}$  and  $\text{W}$ .

A qualitative outline of the bonding in  $\text{M}_2\text{L}_6$  was first given by Albright and Hoffmann.<sup>2</sup> The authors suggested that the observed staggered conformation of  $\text{M}_2\text{L}_6$  is due to steric repulsions between ligands on different metal centers. It was proposed that the eclipsed conformation, favored by electronic factors according to ref 2, would be adopted by  $\text{M}_2\text{L}_6$  for small-size ligands.

It has recently been possible to carry out ab initio calculations on binuclear metal compounds. Kok and Hall<sup>3</sup> have, in connection with a previous work, published results from ab initio calculations on  $\text{Mo}_2\text{H}_6$  and  $\text{Mo}_2(\text{NH}_2)_6$ . They calculated the  $\text{Mo-Mo}$  bond strength  $D(\text{Mo}\equiv\text{Mo})$  in  $\text{Mo}_2\text{H}_6$  to be 118  $\text{kJ mol}^{-1}$  and suggested, based on an error analysis, that a more extensive treatment (larger size configuration interaction) would give  $D(\text{Mo}\equiv\text{Mo})$  as 248  $\text{kJ mol}^{-1}$ . Tentative calculations on  $\text{Mo}_2(\text{NH}_2)_6$  indicated that the replacement of  $L = \text{H}$  with  $L = \text{NH}_2$  might increase  $D(\text{Mo}\equiv\text{Mo})$  further by 117  $\text{kJ mol}^{-1}$ . The best experimental determination<sup>4</sup> of  $D(\text{Mo}\equiv\text{Mo})$ , due to Adedeji et al.,<sup>4</sup> gives

$D(\text{Mo}\equiv\text{Mo})$  as 398  $\text{kJ mol}^{-1}$ . However, the experimental determination of  $D(\text{Mo}\equiv\text{Mo})$  is somewhat hampered by uncertainties in the energy assigned to the  $\text{Mo-L}$  bonds.

Transition metal complexes have been studied extensively by the HFS method first suggested by Slater.<sup>5</sup> One of the most popular implementations of the HFS scheme is the  $X\alpha$ -SW method due to Johnson.<sup>6</sup>

Bursten, Cotton et al.<sup>7</sup> have recently published  $X\alpha$ -SW calculations on  $\text{Mo}_2(\text{NH}_2)_6$ ,  $\text{Mo}(\text{N}(\text{CH}_3)_2)_6$ ,  $\text{Mo}_2(\text{OH})_6$ , and  $\text{Mo}_2(\text{CH}_3)_6$ . They provide a sophisticated analysis of the valence orbitals along with a correlation of calculated and experimental ionization potentials. Bursten et al.<sup>7</sup> dispute that the preferred geometry of  $\text{M}_2\text{L}_6$  for small ligands should be eclipsed. They suggest that electronic factors would prefer a geometry for  $\text{M}_2\text{L}_6$  for the two  $\text{ML}_3$  fragments in a planar trigonal conformation and a free rotation around the metal-metal bond.

The  $X\alpha$ -SW scheme cannot calculate the total electronic energy accurately owing to an approximate representation of the molecular electronic potential. It is for this reason not possible to optimize molecular geometries or calculate bonding energies with the  $X\alpha$ -SW method.

We have used another implementation of the HFS method, due to Baerends et al.,<sup>8</sup> in which the molecular electronic potential

(1) (a) Cotton, F. A. *Acc. Chem. Res.* **1978**, *11*, 225. (b) Chrisholm, M. H.; Cotton, F. A. *Ibid.* **1978**, *11*, 356.

(2) Albright, T. A.; Hoffmann, R. *J. Am. Chem. Soc.* **1978**, *100*, 7736.

(3) Kok, R. A.; Hall, M. B. *Inorg. Chem.* **1983**, *22*, 728.

(4) Adedeji, F. A.; Cavell, K. J.; Cavell, S.; Connor, J. A.; Pilcher, G.; Skinner, H. A.; Safarani-Moattar, M. T. *J. Chem. Soc., Faraday Trans. 1* **1979**, *75*, 603.

(5) Slater, J. C. *Adv. Quantum Chem.* **1972**, *6*, 1.

(6) Johnson, K. H. *J. Chem. Phys.* **1966**, *45*, 3085.

(7) Bursten, B. E.; Cotton, F. A.; Green, J. C.; Seddon, E. A.; Stanley, G. *J. Am. Chem. Soc.* **1980**, *102*, 4579.

(8) (a) Baerends, E. J.; Ellis, D. E.; Ros, P. *Chem. Phys.* **1976**, *2*, 41. (b) Baerends, E. J.; Ros, P. *Int. J. Quantum Chem.* **1978**, *S12*, 169.